Design and performance analysis of a compact magnetic proton recoil spectrometer for DT neutrons*

QI Jian-Min(祁建敏)[1,2;1)] ZHOU Lin(周林)[2] JIANG Shi-Lun(蒋世伦)[2]

[1] Department of Engineering Physics, Tsinghua University, Beijing 100084, China
[2] Institute of Nuclear Physics and Chemistry, CAEP, Mianyang 621900, China

Abstract: A magnetic proton recoil (MPR) spectrometer is a novel instrument with superior performance, including high energy resolution, high count rate and good signal-to-noise ratio (SNR) for measurements of neutron spectra from inertial confinement fusion (ICF) experiments and high power Tokomaks. In this work, the design of a compact MPR spectrometer (cMPR) was evaluated for deuteron-tritium (DT) neutron spectroscopy. The characteristics of the spectrometer were analyzed using 2-D beam transport simulations, 3-D particle transport calculations and Monte-Carlo simulations. Based on the theoretical results, an instrument design that satisfies special experimental requirements is proposed. The energy resolution and efficiency of the spectrometer are also evaluated. The results indicate that the proposed cMPR spectrometer would achieve a detection efficiency and energy resolution of approximately 10^{-8} and 4%, respectively, for DT neutrons.

Key words: magnetic proton recoil (MPR), compact, neutron spectrometer, DT neutron

PACS: 29.30.Hs, 52.70.Nc **DOI:** 10.1088/1674-1137/35/4/010

1 Introduction

Neutron spectra from fusion reactors provide important information about the plasma core region, such as fusion power and ion temperature [1–3]. Neutron spectrometers with performance including high energy resolution, efficiency, count rate and signal-to-noise ratio (SNR) are one of the most important diagnostics for fusion plasma research [4–6]. These spectrometers must maintain a high count rate for data of high statistical accuracy over a large dynamic range because the intensity of fusion neutrons can change by orders of magnitude in a short period of time. Neutrons from large Tokomaks (for example, JET and ITER) are persistent for a relatively long time (∼ms). Thus, neutron spectra can be obtained by detectors capable of discriminating energy in a single-event count mode. However, the lifetime of fusion neutrons from ICF devices and other experiments is extremely short (∼ns); therefore, detectors operating in current-mode are suitable for these conditions. To obtain pulsed neutron spectra, spectrometers based on special methods must be introduced, such as magnetic proton recoil (MPR) and time of flight (TOF) spectrometers. The latter ones are more applicable for deuteron-deuteron (DD) neutrons and have intrinsic limitations on the count rate capability [7].

A MPR spectrometer is a novel instrument with high performance for measurements of neutron spectra from ICF experiments and high power Tokomaks. The first MPR spectrometer was built at JET in 1996 and has been successfully applied in DT experiments [8–10]. The energy resolution of DT neutrons was approximately 2.5% in this spectrometer, and the corresponding efficiency was 5×10^{-5}. The original MPR spectrometer of JET was updated (MPRu) for a better SNR ($>10^4$:1 for DT neutrons in a single-event count mode) [6]. A similar spectrometer, called the "MRS", was built at OMEGA and NIF [11], which achieved an energy resolution of 3% and a corresponding detection efficiency of 10^{-9} with a good SNR (∼ 10:1 for pulsed DT neutrons). Both of the proposed spectrometers are special-purpose equipment.

A compact MPR (cMPR) spectrometer dedicated to DT neutron spectroscopy in various environments

Received 15 July 2010, Revised 25 August 2010
* Supported by Science and Technology Development Foundation of China Academy of Engineering Physics (2008B0103003)
1) E-mail: qjm06@mails.tsinghua.edu.cn

(in limited space, such as an accelerator hall and intense pulsed fusion neutron facilities) is currently under construction. It is expected to achieve a sufficient detection efficiency ($\sim 10^{-8}$ counts per n/cm^2) since the objective neutron yields are high ($> 10^{10}$ s^{-1} for steady state neutrons, and $> 10^{13}$ s^{-1} for pulsed neutrons). At the same time, an energy resolution of approximately 3%–6% with a good SNR ($\sim$10∶1) is required for current applications in different experimental environments. Moreover, the spectrometer requires a compact structure, low weight and low cost, as well as optimal spectrometer shielding and electronic design to improve the SNR.

2 Design of the cMPR spectrometer

A typical MPR spectrometer can be divided into three independent components: a neutron-to-proton (n-p) conversion system, a magnetic analysis system and focal plane detectors. Together, these components allow the spectrometer to transfer an incident neutron spectrum ($S_n(E_n)$) to a recoil proton spectrum ($S_p(E_p)$) to a focal plane distribution of recoil protons ($I_p(x')$). Each of the three elements can be designed, simulated and studied individually. A schematic view of the principle of the cMPR spectrometer is shown in Fig. 1.

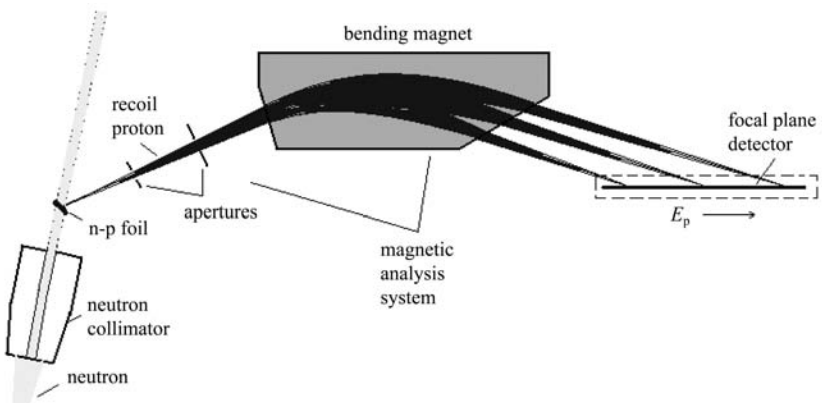

Fig. 1. Principle of the proposed cMPR spectrometer.

2.1 The n-p conversion system

The n-p conversion system consists of a neutron collimator and a n-p recoil foil. Recoil protons are produced in elastic scattering reactions between incident neutrons and hydrogen nuclei in a thin polyethylene film, called a recoil foil or proton radiator. The energy of the recoil proton (E_p) is determined by both the neutron energy (E_n) and the recoil angle (θ_{np}),

$$E_p = E_n \cdot \cos^2 \theta_{np} \,. \quad (1)$$

For mono-energetic neutrons, a large recoil angle will reduce the energy of the corresponding recoil protons. Hence, a small bending magnet can be employed to achieve a compact design. The incident neutrons and selected protons are separated concomitantly, and the magnetic analysis system and focal plane detectors are protected from direct irradiation of incident neutrons.

The elastic scattering cross-section (σ_s, barns) between neutrons and hydrogen nuclei changes as the neutron energy varies (E_n = 0.1–35 MeV) [12],

$$\begin{aligned}\sigma_s(E_n) = & \, 3\pi/[1.206E_n + (-1.86000 \\ & +0.09415E_n + 0.00013E_n^2)] \\ & +\pi/[1.206E_n + (0.4223 + 0.1300E_n)^2]. \quad (2)\end{aligned}$$

The detection efficiency (ε_{np}) of the proton recoil method is determined by the characteristics of the recoil foil, including the elastic scattering cross-section and the thickness of the foil. The protons lose energy in the foil due to ionization effects. The width (ΔE_p) of the energy distribution of recoil protons at the chosen angle is determined by the foil thickness and the proton stopping power of polyethylene [13]. To force the recoil protons to follow a trajectory that is perpendicular to the foil surface in order to minimize energy loss, the n-p foil was inclined with respect to the neutron incident direction. At a recoil angle of 45°, the change in proton energy broadening, ΔE_p, and the efficiency, ε_{np}, as a function of foil thickness are shown in Fig. 2, using proton stopping power data of polyethylene from PSTAR [14]. A thin foil can reduce energy broadening in the recoil foil to improve the energy resolution of the spectrometer, but would also decrease the detection efficiency. To achieve a compact design, a recoil angle of 45° and a foil thickness of 2–4 mg/cm^2 were selected.

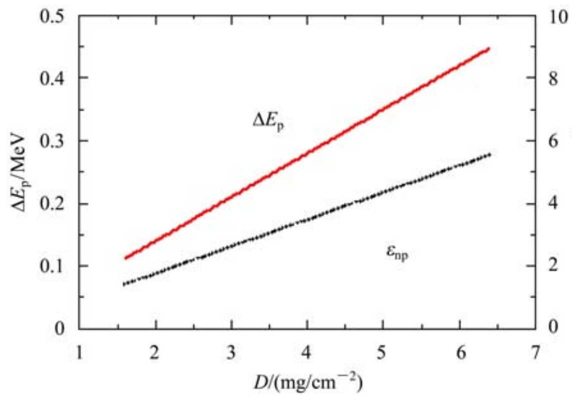

Fig. 2. Proton energy broadening and the change in n-p efficiency as a function of foil thickness, D. The incident neutron energy was 14 MeV and the recoil angle was 45°.

2.2 The magnetic analysis system

As shown in Fig. 3, the magnetic analysis system includes proton apertures, which determine the beam incidence geometry, and a bending magnet, which provides the necessary magnetic field for energy dispersion of recoil protons. Recoil protons of different energies are dispersed and focused at different positions on the focal plane, and a MPR spectrometer can be applied to measure the spectrum of either steady-state or pulsed DT neutrons.

The basic design of the magnetic analysis system was founded on the 2-D beam transport code, "TRANSPORT" [15]. To minimize the size of the spectrometer and to fulfill performance requirements, a small rotation angle and a reasonably short target length and focus length were selected. Thus, the volume of the cMPR spectrometer will be approximately 1.8 m × 0.8 m × 0.8 m. The optimized design was accomplished by simulating an accurate model of the system (shown in Fig. 3) using a 3-D charged particle transport code, which is based on an "ab initio" calculation of charged particles in a magnetic field.

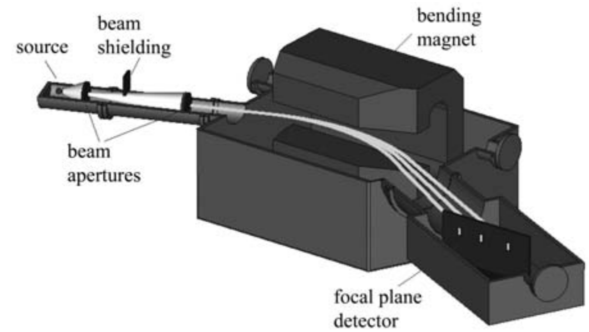

Fig. 3. Precise model of the magnetic analysis system.

The 7.9 kG dipole magnet with dimensions of 42 cm × 26 cm × 29 cm and a weight of approximately 190 kg was constructed, as shown in Fig. 4 (left). A high performance material (NdFeB) was employed in the bending magnet to improve the performance. To increase the vertical magnetic field strength in the magnet air gap and to extend the region of uniformity, the magnet design was optimized with a 3D electromagnetism emulator. The height of the magnet air gap determines the maximum solid angle of incidence, and a height of 3 cm was selected for the magnetic analysis system. The measured distribution of the magnetic field on the central plane of the air gap is shown in Fig. 4 (right), where the center of the graph illustrates an area with a magnetic field non-uniformity of less than 1%.

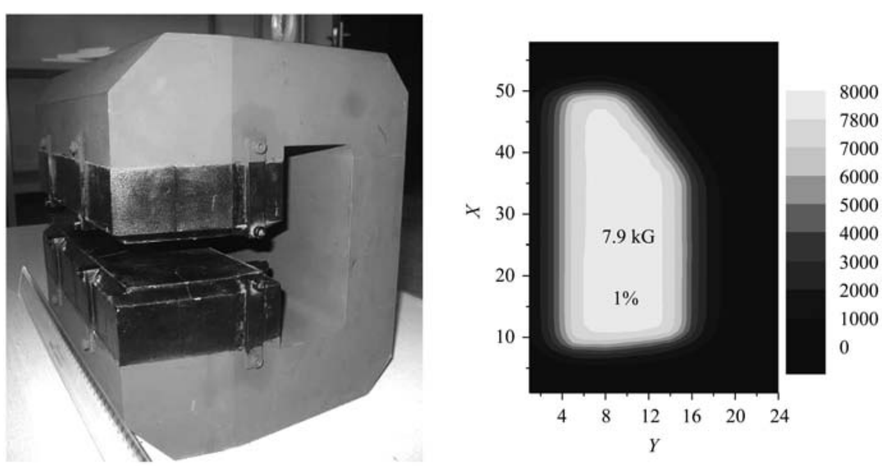

Fig. 4. The bending magnet (left) and the measured magnetic field strength distribution on the central plane (right).

Double apertures with rectangular holes for proton collimation were introduced into the spectrometer, as shown in Fig. 5. The C1 aperture was located near the n-p recoil foil, and the dimensions of the aperture were equal to the effective dimensions of the recoil foil (L_x for horizontal dimension and L_z for vertical dimension). The distance (L_1) between C1 and the entrance to the magnet was equal to the target length. The solid angle was determined by the size of the apertures and the distance (L_a) between them.

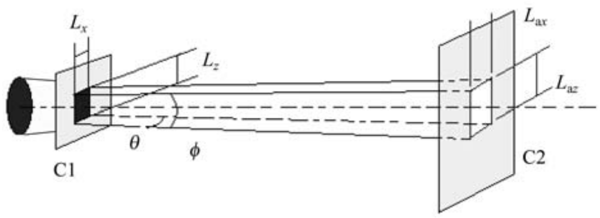

Fig. 5. Proton collimation with double apertures.

2.3 Focal plane detectors

Either single-event mode or current-mode detectors can be employed as focal plane detectors in a MPR spectrometer. Single-event mode detectors provide measurements of "steady-state" neutrons, while current-mode detectors provide measurements of pulsed neutrons. Both types of detectors must be able to detect protons with an efficiency of approximately 100% and must not be sensitive to background noise.

The cMPR spectrometer is expected to measure neutrons with an energy between 8–16 MeV and the energy range of recoil protons is between 4 to 8 MeV. The detector array will consist of 3 background detectors and 30 signal detectors, each of which covers 3.2% of the total energy range (130 keV). The array will be based on Si-PIN semiconductor detectors, where the sensitivity of each detector is determined by both the proton range in silicon and the depth of detector sensitive volume. The focal plane detectors will be able to operate in single-event mode and current-mode. By implementing effective shielding and electronic background reduction methods, the SNR of the spectrometer will be improved to better than 10∶1 for pulsed neutron measurements. A detailed design of the electronics of the system and relevant analytical calculations are currently being developed.

3 Performance analysis

Fusion neutron spectra obtained from a typical MPR spectrometer are based on the magnetic analysis of proton energy. Neutron energy measurements are obtained by converting neutrons into recoil protons and detecting their energy distribution. These steps are separated from each other and can be calculated and calibrated individually.

3.1 Characteristics of the magnetic analysis system

Using a magnetic analysis system, the recoil protons from the recoil foil were dispersed and focused onto the focal plane according to their energy. The distribution of proton energies was subsequently converted into a distribution of focal plane positions.

The resolution of particle positions along the focal plane is considered as the primary characteristic of the magnetic analysis system. The relationship between the energy and the position of the recoil protons is determined by the magnetic analysis. The focal plane was evaluated by 3D charged particle transport calculations and experimental calibrations. Protons and α particles with the same kinetic energy follow an identical path in a given magnetic field. Thus, the system can be calibrated with known mono-energetic α particles from radioactive sources, such as ^{239}Pu and ^{226}Ra. The widths of the distributions can be obtained by repositioning CR-39 track detectors and the focal points of α particles at different energies can be subsequently determined. An experimental determination of the focal point of α particles from ^{239}Pu is shown in Fig. 6.

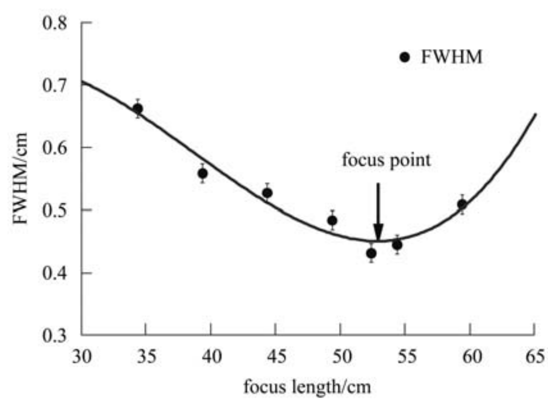

Fig. 6. Experimental determination of the focal point of α particles from ^{239}Pu at an energy of 5.155 MeV. The uncertainty of FWHM was ±0.2 mm.

A precise model of the magnetic analysis system (Fig. 3) was simulated with a 3-D charged particle transport code. The magnetic system that was constructed can analyze protons with an energy between 3.3 to 8.6 MeV; thus, the neutron detection range of the cMPR spectrometer is 6.6–17.2 MeV. For the selected focal plane and system configuration, the distribution center (x', cm) of recoil protons on the focal plane increased linearly with proton energy (Fig. 7), which is derived from both the simulation and experiment results. Therefore, the relationship between the energy and position of the protons was described by

$$\mathrm{d}E_\mathrm{p}/\mathrm{d}x' = 0.125\ \mathrm{MeV/cm}\,, \tag{3}$$

which means that the energy dispersion of 7 MeV protons on the focal plane is 5.6 mm per $\Delta E_\mathrm{p}/E_\mathrm{p} = 1\%$. Moreover, energy broadening (ΔE_m) of monoenergetic protons due to magnetic analysis is

$$\Delta E_\mathrm{m} = \mathrm{FWHM}\,(x') \cdot \mathrm{d}E_\mathrm{p}/\mathrm{d}x'\,, \tag{4}$$

where FWHM(x') is the full width of the focal plane distribution at half maximum.

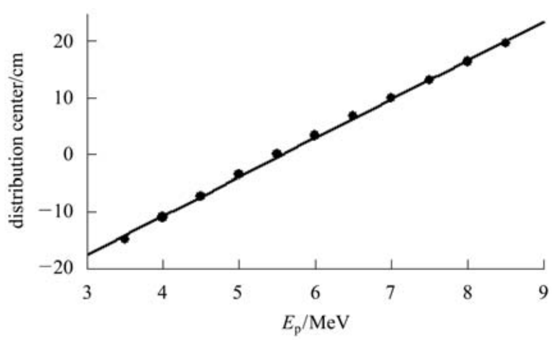

Fig. 7. Distribution centers of recoil protons on the focal plane as a function of energy, derived from both the simulation and experimental results.

FWHM(x') can be adjusted by changing the incidence geometry of the magnetic system. The proton incidence solid angle (Ω_p) of the system is determined by the configuration of double-aperture collimation,

$$\Omega_\mathrm{p} = A_\mathrm{C2}/L_\mathrm{a}^2\,, \tag{5}$$

where A_C2 is the area of aperture C2 in cm^2 and L_a is the distance between aperture C1 and C2 in cm, as shown in Fig. 5. Given the current configuration of the bending magnet air gap, the incidence solid angle varies between 0.3 and 0.9 msr. The measured position distribution at the focus point of 5.155 MeV α particles from a ^{239}Pu source in different aperture configurations is shown in Fig. 8. The energy broadenings (ΔE_m) under different aperture configurations are 162 keV, 143 keV and 112 keV, respectively. In these experiments, CR-39 detectors were employed and the uncertainty of position detection was ±0.2 mm. The width and peak area of the distribution decrease with a decrease in aperture size, which leads to an improved energy resolution and a decreased detection efficiency.

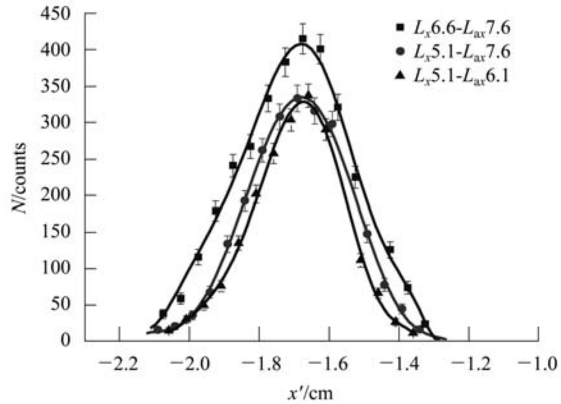

Fig. 8. Distributions of 5.155 MeV α particles from a ^{239}Pu source at the focus point under different aperture configurations. The apertures possessed the following dimensions: L_x = 6.6 mm, L_{ax} = 7.6 mm; L_x = 5.1 mm, L_{ax} = 7.6 mm; L_x = 5.1 mm, L_{ax} = 6.1 mm and L_a = 26 cm. The uncertainty of position detection was ±0.2 mm.

3.2 Efficiency

The conversion of neutrons to recoil protons was determined by the system geometry and the cross section of n-p scattering. The angular distribution ($\sigma_\mathrm{s}(E_\mathrm{n},\ \theta_\mathrm{np})$, barn) of the cross section of n-p scattering in the reference frame is not isotropic if $E_\mathrm{n} >$ 10 MeV [11],

$$\begin{aligned}\sigma_\mathrm{s}(E_\mathrm{n},\theta_\mathrm{np}) \;=\; & (\cos\theta_\mathrm{np}/\pi)\cdot\sigma_\mathrm{s}(E_\mathrm{n}) \\ & \cdot[1+2(E_\mathrm{n}/90)^2\cos^2(2\theta_\mathrm{np})] \\ & /[1+2(E_\mathrm{n}/90)^2/3].\end{aligned} \tag{6}$$

The last term in the equation is the anisotropic factor. For neutrons with an energy of 14 MeV, the anisotropic factor is 0.984 at $\theta_\mathrm{np} = 45°$. The spectrometer efficiency (ε) is described by

$$\varepsilon \approx (\cos\theta_\mathrm{np}/\pi)\cdot\varepsilon_\mathrm{np}\cdot\Omega_\mathrm{p}\cdot\varepsilon_\mathrm{d}\,, \tag{7}$$

where ε_d is the efficiency of the focal plane detectors, which is typically close to 100%.

The efficiency of the spectrometer can be adjusted by ε_np and Ω_p, which are determined by the n-p foil thickness and the geometry of the magnetic analysis system. For neutrons with an energy of 14 MeV and a foil thickness between 2 to 4 mg/cm^2 (to keep good energy resolution), the n-p efficiency ε_np is approximately 1.5–4.0×10^{-4} (Fig. 2). The incidence solid angle of the magnetic system, Ω_p, is approximately 0.3–0.9 msr in the current design, and the total efficiency is about 1.2–5.7×10^{-8} (Fig. 9).

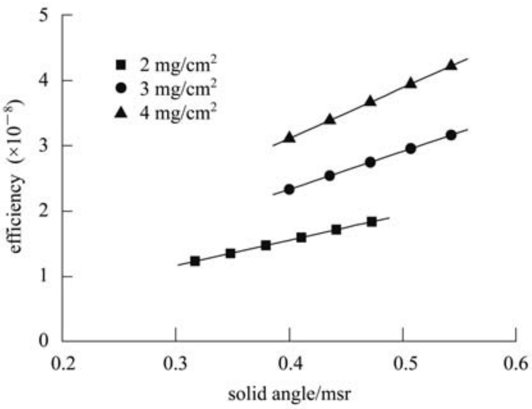

Fig. 9. Efficiency of the cMPR spectrometer as a function of foil thickness and Ω_p.

3.3 Energy resolution

The energy distribution of recoil protons emitted from the n-p foil is almost rectangular for mono-energetic neutrons. The width (ΔE_p) is determined by the proton stopping power of the polyethylene and the thickness of the recoil foil. The horizontal dimensions of the apertures broaden the range of recoil angle, which leads to kinematic energy broadening (ΔE_C) of recoil protons at a given angle (see Eq. (1)). As a result, protons generated by mono-energetic neutrons enter the magnetic analysis system with an energy distribution that has a width determined by ΔE_p and ΔE_C. The energy distribution of recoil protons corresponding to 14 MeV neutrons was evaluated as a function of foil thickness and the incident solid angle of the magnetic analysis system, as shown in Fig. 10, by using a Geant4 simulation. The distribution of protons was centered at 6.865 MeV and 6.932 MeV with a foil thickness of 2 mg/cm^2 and 4 mg/cm^2, respectively. The distribution widths were 0.313 MeV, 0.368 MeV, and 0.382 MeV for the three configurations.

The total proton energy broadening (ΔE_t) of mono-energetic neutrons is determined by ΔE_p, ΔE_C, and ΔE_m. As shown in Table 1, the performance of the spectrometer was evaluated under different conditions, based on both the theoretical and the experimental results described above. The corresponding distributions of protons on the focal plane are provided in Fig. 11. These were obtained from Monte Carlo simulations and 3D charged particle transport calculations. Energy broadening caused by the magnetic analysis system (ΔE_m) did not significantly contribute to the total energy broadening of the spectrometer (ΔE_t). This result indicates that the magnetic analysis system displays satisfactory performance and the total energy broadening was mainly dependent on the recoil foil (ΔE_p) and the apertures (ΔE_C). In other words, the energy resolution of the cMPR spectrometer is limited by the method of proton recoil. The applied calculation and simulation methods are also evaluated by calculating a simple model of the MRS spectrometer of OMEGA and NIF [16].

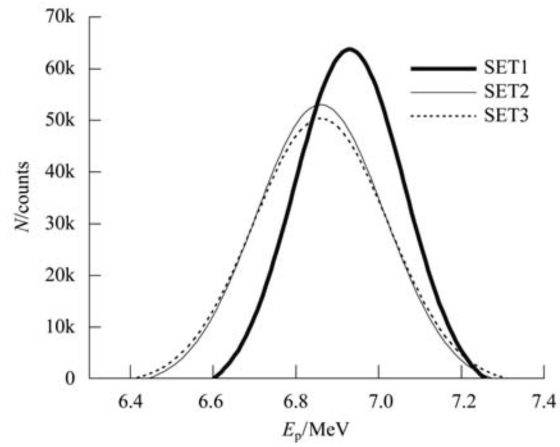

Fig. 10. Proton energy distributions for neutrons with an energy of 14 MeV and a 45° recoil angle. SET1: D = 2 mg/cm^2, Ω_p = 0.43 msr; SET2: D = 4 mg/cm^2, Ω_p = 0.43 msr; SET3: D = 4 mg/cm^2, Ω_p = 0.5 msr.

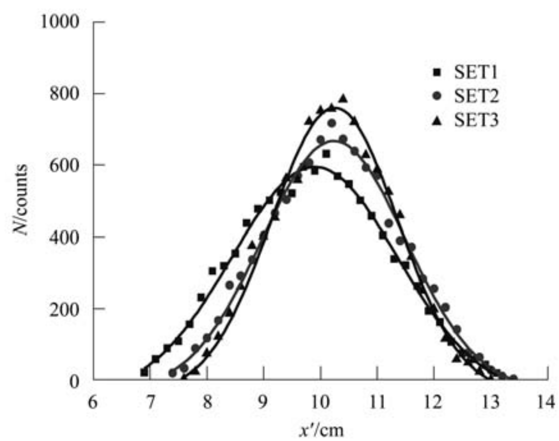

Fig. 11. The calculated distribution of recoil protons on the focal plane under different conditions (shown in Table 1) for 14 MeV neutrons.

The energy resolution of the cMPR spectrometer is between 3%–6% and the corresponding efficiency is between (0.9–4.0)$\times10^{-8}$, which can be adjusted by changing the recoil foil thickness and the aperture size. This result is in accordance with the MRS spectrometer of OMEGA and NIF if choosing a prior design for energy resolution. The energy resolution can be improved by reducing the efficiency or applying an advanced method of spectral analysis. A thinner foil (for example, 2 mg/cm^2) can improve the spectrometer resolution while still maintaining efficiency near 10^{-8}. Smaller apertures and longer distances can also improve the spectrometer resolution, but result in a reduced efficiency. Therefore, a trade-off between spectrometer resolution and efficiency is necessary for different experimental requirements.

Table 1. Energy resolution and efficiency of the cMPR for 14 MeV neutrons as a function of experimental parameters.

SET	foil thickness/(mg·cm^{-2})	apertures distance/cm	C1		C2	
			L_x/mm	L_z/mm	L_{ax}/mm	L_{az}/mm
1	4	28	6.6	5.6	7.1	5.6
2	2	30	5.6	5.6	6.1	5.6
3	2	30	5.1	5.6	5.1	5.6

energy broadening				efficiency/(10^{-8})	resolution (%)
$\Delta E_{\rm p}$/MeV	$\Delta E_{\rm C}$/MeV	$\Delta E_{\rm m}$/MeV	$\Delta E_{\rm t}$/MeV		
0.28	0.29	0.18	0.46	4.0	6.6
0.14	0.27	0.15	0.36	1.5	5.1
0.14	0.24	0.13	0.29	1.2	4.2

4 Conclusions

A conceptual design for a compact MPR spectrometer dedicated to pulsed DT neutron spectroscopy under different experimental conditions is presented. Three components of the spectrometer were simulated and the relationships between spectrometer parameters and performance were studied through Monte Carlo simulations and 3D charged particle transport calculations. The results indicate that the resolution and efficiency of the cMPR spectrometer are mainly dependent on the design of the recoil foil and apertures, which can also be adjusted by varying the foil thickness and aperture dimensions. The magnetic analysis system, which is the hard core of the cMPR spectrometer, achieved satisfactory performance, and the proposed cMPR spectrometer will achieve an energy resolution of approximately 3%–6% and a corresponding efficiency of better than 10^{-8} for DT neutrons. The cMPR spectrometer will be approximately $1.8\ \text{m}\times 0.8\ \text{m}\times 0.8\ \text{m}$ while the total weight will be less than 350 kg. Thus, it is relatively compact and fulfills the design goals. A detailed design of spectrometer electronics and relevant analytical calculations are currently being developed. The characteristics of the proposed spectrometer with accelerated DT neutrons will be evaluated in a future study.

References

1 Jarvis O N. Nucl. Instrum. Methods A, 2002, **476**: 474–478
2 Källne J, Ballabio L, Conroy S et al. Rev. Sci. Instrum., 1999, **70**(1): 1181–1184
3 Aymar R. Fusion Engineering and Design, 2002, **61-62**: 5–8
4 Tardocchi M, Gorini G, Andersson S E et al. Rev. Sci. Instrum., 2006, **77**: 126107
5 Sjöstrand H, Giacomelli L, Andersson S E et al. Rev. Sci. Instrum., 2006, **77**: 10E717
6 Giacomelli L, Hjalmarsson A, Sjöstrand H et al. Nucl. Fusion, 2005, **45**: 1191–1194
7 Källne J, Gorini G. Rev. Sci. Instrum., 1993, **64**(10): 2765–2768
8 Maas A C, Andrew P, Coad P et al. Fusion Engineering and Design, 1999, **47**: 247–251
9 Frenje J, Ballabio L, Conroy S et al. Rev. Sci. Instrum., 1999, **70**(1): 1176–1180
10 Frenje J, Green K M, Hicks D G et al. Rev. Sci. Instrum., 2001, **72**(1): 854–858
11 Glebov Y V, Meyerhofer D D, Sangster T C et al. Rev. Sci. Instrum., 2006, **77**: 10E715
12 JI Chang-Song. Handbook of Nuclear Radiation Detectors & Their Experiment Techniques. Beijing: Atomic Energy Press, 1990. 168–172 (in Chinese)
13 JI Chang-Song. Neutron Detection Periment Method. Beijing: Atomic Energy Press, 1998. 210–212 (in Chinese)
14 Berger J M, Coursey S J, Zucker A M et al. Stopping-Power and Range Tables for Electrons, Protons, and Helium Ions, 2005 // http://www.nist.gov/physlab/data/star/index.cfm
15 PSI Graphic Transport Framework by U. Rohrer based on a CERN-SLAC-FERMILAB version by K.L. Brown et al
16 Hawkes N P, Belle P, Bond D S et al. Rev. Sci. Instrum. 1999, **70**(1): 1134–1138